The Meteoritical Society

Meteoritics & Planetary Science 44, Nr 11, 1707–1715 (2009)
Abstract available online at http://meteoritics.org

Stardust glass: Indigenous and modified comet Wild 2 particles

Frans J. M. RIETMEIJER

Department of Earth and Planetary Sciences, MSC 03-2040, University of New Mexico, Albuquerque, New Mexico 87131–0001, USA
*Corresponding author. E-mail: fransjmr@unm.edu

(Received 22 June 2009; revision accepted 08 August 2009)

Abstract–Does comet 81P/ Wild 2 have indigenous glass? Glass is used here to include all types of amorphous materials that could be either indigenous or modified comet Wild 2 grains, and all amorphous phases in chondritic aggregate interplanetary dust particles (IDPs). The answer is that it probably does, but very little is known of their compositions to allow a definitive answer to be given. There is no evidence among the collected comet dust for interstellar glass with embedded metals and sulfides. There is, however, ample evidence for melting of the smallest, sub-micrometer comet particles of nanometer-scale grains similar to those in the matrix of chondritic aggregate IDPs, including pyrrhotite. Massive patches of Mg-SiO, Al-SiO, or Ca-Si-O glass are incorporated in the familiar, vesicular Si-rich glass are melted Wild 2 silicates. Magnesiosilica glass has a deep metastable eutectic smectite-dehydroxylate composition. It indicates that very high temperatures well above the liquidus temperatures of forsterite were achieved very rapidly and were followed but ultra-rapid quenching. This predictable and systematic response is not limited to Mg-silicates, and recognizing this phenomenon among massive glass will provide a means to complete the reconstruction of this comet's original minerals, as well as constrain the physiochemical environment created during aerogel melting and evaporation.

INTRODUCTION

Do comet nuclei contain crystalline silicates, viz. forsterite and enstatite, or do they only contain amorphous silicates (hereafter called silicate glass, or glass). The questions can be addressed by laboratory analyses of comet nucleus samples such as collected by the Stardust mission. Glasses are metastable solids that are sensitive to glass-in-glass separation and crystallization. In comets, the glass to crystalline dust ratio can be an indicator of comet aging (Nuth et al. 2000a). Forsterite and enstatite in comets might evolve during thermal processing of magnesiosilica glass (Hallenbeck et al. 1998, Fabian et al. 2000) and refractory minerals might potentially evolve from aging of Ca,Mg,Fe-bearing aluminosilica glasses (Rietmeijer 2002). Mineralogical analyses of comet 81P/Wild 2 (hereafter Wild 2) particles captured in the Stardust under-dense aerogel at 6.1 km s^{-1} revealed a comet with a richness of crystalline silicates and a wide variety of high-temperature minerals (Brownlee et al. 2006; Zolensky et al. 2006). A caveat is that the Stardust mission and the Deep Impact mission (Lisse et al. 2006) showed the above only for Jupiter-family comets but not for Halley-type comets. Another caveat is that most crystalline Wild 2 silicates are in the micrometer range including terminal particles of refractory CAI-like minerals and chondrule-like objects (Zolensky et al. 2006, 2008; Nakamura et al. 2008a) that might have been transported from inner part of the solar nebula to the Kuiper belt (Brownlee et al. 2007; Ciesla 2007). Was it also the case for the nanometer-scale Wild 2 grains, or could they be the common early solar system dust that included interstellar silicates? This time the issue is whether comet Wild 2 contains indigenous silicate glasses or whether glasses captured in aerogel were formed in situ. The chondritic porous (CP), interplanetary dust particles (IDPs) are thought to be debris from active comets (Brownlee 1978; Bradley and Brownlee 1986) and they serve as a guide to address this issue (Ishii et al. 2008). Although a survey of 42 low (<14 km s^{-1}), intermediate (14–18 km s^{-1}) and high (>18–21 km s^{-1}) velocity IDPs found systematic differences between low- and high-velocity IDPs, it was also found that it can be difficult to unambiguously classify an individual IDP as an asteroidal particle or a cometary IDP because textural and mineralogical characteristics of each group can be found within the other (Joswiak et al. 2000). Anhydrous CP IDPs do not appear to be restricted to high-velocity, presumably, cometary IDPs. This entire range of entry velocities (Brownlee et al. 1994, 1995) is typical for asteroidal meteors (cf. Rietmeijer 2000) that after the discovery of comets in the outer asteroid belt (Hsieh and Jewitt 2006) could yield cometary IDPs. Still, the sources of chondritic aggregate IDPs remain unknown but since their textures and petrological properties are entirely different from these properties of any meteorites in our collections, they are from small solar system bodies that are not parent bodies of these meteorites (Mackinnon and Rietmeijer 1987). Some IDPs might be affiliated with CI parent bodies (Rietmeijer 2004a).

Chondritic aggregate IDPs are assemblages of a limited number of size-binned grain types. The matrix is an agglomerate of ferromagnesiosilica grains <500 nm in diameter that (1) have an amorphous matrix with numerous nanometer scale Fe,Ni-sulfide and Fe,Ni-metal grains (Bradley 1994; Bradley and Ishii 2008), known as GEMS (glass with embedded metals and sulfides; Bradley 1994), or (2) consist of three phases, viz. Si-rich glass, olivine and pyroxene (Rietmeijer 2002, 2009a). The matrix is host to variable amounts of ~1 to ~5 micron Mg-rich olivine, Ca-free and low-Ca pyroxene, and Ca-rich pyroxene, Ni-free and low-Ni pyrrhotite, Si-rich glass grains and rare SiO_2 minerals (Brownlee 1985; Bradley et al. 1988; Rietmeijer 1998, 2009a). Aggregate porosity ranges from chondritic porous (>80% porosity) IDPs to more compact aggregates (Rietmeijer 1998); within aggregates there could be non-porous compound grains <1 μm (Rietmeijer 2009a) such as "first accretionary particles" (Brownlee and Joswiak 2004) of amorphous silicate, forsterite, enstatite, FeS, GEMS, and organic materials.

The under-dense, density-graded (0.02–0.05 g/cc) silica aerogel is a solid substance wherein tiny spheres of bonded silicon and oxygen atoms are joined into long strands separated by pockets of air. It was designed for "intact capture" of ~10 μm-sized comet Wild 2 grains that entered aerogel at 6.1 km/s (Tsou et al. 2003). It worked very well. Intact survival of smaller grains was less likely and would be a function of their deceleration rates, among others. Survival does not mean that grains were not heated; only that temperatures did not exceed their melting point. Nanometer comet particles would not survive except under unusual conditions such as shielding fine-grained material in the wake of the massive compound FeS-enstatite terminal particle T57 (Brownlee et al. 2006). It has been suggested that such fine-grained material at the front and on the sides of a massive terminal particle could spall off during deceleration and collect in its wake.

Most of the nanometer-scale grains melted and commingled with impure silica melt in 10–20 μm-sized, irregular clumps located in the bulbous part of type B and C deceleration tracks (cf. Hörz et al. 2006). These clumps are vesicular Si-rich glass with numerous nanometer scale Fe-Ni-S compound grains and "dust-rich areas," Mg-rich silicates, e.g., forsterite (<500 nm), "FeS" (<100 nm) and GEMS-like objects (Leroux et al. 2008; Nakamura et al. 2008b; Tomeoka et al. 2008; Zolensky et al. 2008). GEMS-like objects are found embedded in flight aerogel (Keller et al. 2006; Zolensky et al. 2006, 2008; Ishii et al. 2008).

I will use the chemical and petrological properties of various glasses in compact aerogel and compare these properties to components in chondritic aggregate IDP L2011A9 that serves as an analog. All data presented here are from published sources, including the Stardust Preliminary Examination Team phase, wherein details on analytical techniques and procedure can be found, especially the supplemental information in the paper by Zolensky et al. (2006).

GEMS-LIKE OBJECTS

The matrix of chondritic aggregate IDPs is often dominated by spherical grains with an amorphous ferromagnesiosilica matrix of highly variable Mg/(Mg + Fe) (*mg*) ratios with many Fe,Ni-sulfide and Fe,Ni-metal, and also Fe,Ni-oxide, grains typically <15 nm. The petrographic description of these grains as glass with embedded metals and sulfides covers (1) "real" GEMS (Bradley 1994; Bradley and Ishii 2008) and (2) ultrafine-grained (ufg) principal components (PCs) (Rietmeijer 1998, 2002, 2009a). The difference is their hypothesized mode of formation, viz. (1) pre-accretionary irradiation-induced amorphization for 'real' GEMS (Bradley 1994), and (2) evolved non-equilibrium condensates (Rietmeijer 2002; Rietmeijer and Nuth 2007; Rietmeijer et al. 1999), respectively. Subsequently Keller and Messenger (2004) also proposed the latter origin when arguing for solar system GEMS and ISM-candidate GEMS. Keller and Messenger (2004) submitted that solar system GEMS do not have a solar elemental composition, which is consistent with earlier proposals (Rietmeijer 2002), and that interstellar medium-candidate GEMS are S-depleted. For the purpose of this paper, the acronym GEMS will be used for both "real" GEMS and ufg PCs. Unambiguous proof for GEMS indigenous comet to Wild 2 would bolster their hypothesized pre-accretionary, and hence their interstellar origin but proof that their petrographic properties are uniquely caused by irradiation-induced amorphization is still lacking. Thus, there is no distinction between interstellar GEMS and evolved condensates based on petrographic properties. Interstellar GEMS might be recognized when they contain crystalline relict grains, mostly Fe-sulfide but also olivine and FeNi-metal or AlSiO-glass (Bradley et al. 1998). Zolensky et al. (2006) concluded that GEMS-like objects in compressed Stardust flight aerogel could be either indigenous comet GEMS or have formed as a result of intermingling of melted fine-grained Wild 2 particles and melted aerogel. GEMS-like objects with relict grains were not found yet in flight aerogel which leaves composition as the only a potential diagnostic signature.

Pre-flight silica aerogel is not 100% pure silica but contains various ppm and ppb levels of contaminant elements (Tsou et al. 2003). Some of these elements at the percent level occur in the compressed flight aerogel (Table 1), which is consistent with other reports of impure flight aerogel (Rietmeijer 2009b). The remarkable similarity between the Fe- and CI-normalized distribution patterns in pre-flight and flown aerogel (Fig. 1) is interpreted as a flight-aerogel background (Rietmeijer 2009b). When molten Wild 2 particles and aerogel commingled during capture, the aerogel background contaminants were inherited and concentrated due to a volume change from under-dense aerogel to shock-compressed silica melt prior to quenching into Si-rich vesicular glass. It remains to be determined whether this background is a track-specific or not.

A comparison of the means and standard deviations of 46 GEMS-like objects from four Stardust tracks (Table 1) and the flight aerogel background values (Table 1) reveals that the element abundances of these objects cannot be distinguished from background values. Still, the electron opaque inclusions are real which leaves three possibilities, viz. (1) a fraction of Fe, Ni and S is attributable to comet sulfide grains, (2) the inclusions were tiny immiscible liquid droplets in silica melt with background contaminants, or a combination of both. The GEMS-like object that was produced in a hypervelocity capture experiment of pyrrhotite in Stardust aerogel is a convincing demonstration that these objects can be caused by micrometer-sized pyrrhotite grains (Ishii et al. 2008). The low abundances of Mg, Al, Ca, Cr, and Mn (Table 1) in the silica glass are then consistent with a background. Notwithstanding the textural similarities, a Student's t-test of the means for GEMS in CP IDPs and the GEMS-like objects show they are for different populations despite overlapping Mg and Fe abundances (Fig. 2). The Mg versus Fe (at) diagram represents the compositional variation of these Si-rich objects that may also contain low amounts of Al, S, Ca, Cr, Mn, and Ni. In this diagram pure silica plots in its origin. Composition alone cannot identify GEMS at low Fe and Mg contents. GEMS-like objects that are associated with Si-rich vesicular glass in allocation C2092,2,80,46,1 also plot in the low-Mg/low, Fe region (Fig. 2). Its parent ~20 µm-size clump was extracted flight from aerogel near the entrance hole of the bulbous type B track C2092,2,80. They occur in a different context than most GEMS-like objects that are embedded in (compressed) flight aerogel but their compositions are indistinguishable from the other GEMS-like objects. For comparison Figure 2 also shows the compositional heterogeneity of the Si-rich vesicular glass in the same allocation. Vesicular glass and the GEMS-like object compositions with Fe <10 (at) overlap. The wide range of Fe-contents in the vesicular glass (Fig. 2) reflects primarily variations in the spatial density of very small Fe-Ni-S inclusions, variable grain sizes of the inclusions, or both (Fig. 3). There is also a contribution from Mg,Fe-silicates. The cause of the variable density and sizes of these inclusions is still not known. There are two relevant observations, viz. (1) this glass clump was extracted close to the track's entrance hole, and (2) this track is classified as a bulbous type B track on the NASA Stardust website, but Hörz et al. (2006) showed it as an example of a bulbous type C track caused by hypervelocity capture of a volatile rich Wild 2 particle. A dynamic impact environment might have caused the spallation of small heterogeneous Wild 2 agglomerates and the formation a spray of small immiscible liquid "sulfide" spheres. The chemical signatures of Wild 2 grains preserved in vesicular glass are consistent with cometary agglomerates that resembled the matrix of chondritic aggregate IDPs, including pyrrhotite (Rietmeijer 2009a). A pyrrhotite grain in a Wild 2 agglomerate (cf. Ishii et al. 2008) might have caused the GEMS-like object in Fig. 3 which lost its distinctive outline by assimilation in surrounding Si-rich glass.

Table 1. Mean atomic % abundances of 46 GEMS-like objects in Stardust (source: Ishii et al. 2008; Table 1) and the flight aerogel background measured in allocation C2092,2,80,47 (source: Rietmeijer 2009b).

	Mean ± S.D.	Stardust background
Mg	2.05 ± 1.83	0.6
Al	1.42 ± 1.27	0.2
Si	24.44 ± 4.24	No data
S	1.13 ± 2.34	0.4
Ca	1.47 ± 2.54	0.05
Cr	0.00 ± 0.00	0.1
Mn	0.00 ± 0.03	0.06
Fe	2.79 ± 3.02	2.4
Ni	0.12 ± 0.26	0.4

GEMS (Bradley 1994) in aggregate IDPs were hypothesized to be interstellar amorphous silicate (Bradley and Ishii 2008). This origin was challenged (Martin 1995; Min et al. 2007). When GEMS-like objects were found in compressed Stardust flight aerogel it became a contentious issue. It appears that identifying intact-captured interstellar GEMS from comet Wild 2 remains a very difficult challenge. The petrographic textures and compositions of GEMS-like objects are indistinguishable from vesicular glass compositions (Fig. 2). Their compositions are mostly different from GEMS in CP IDPs (Fig. 2).

Mg,Al,Ca-GLASS

Another type of Stardust glass occurs as compact, amorphous "dust-rich areas" <1 µm that are frequently separated by several micrometers in vesicular glass (Leroux et al. 2008). Similar massive patches may occur between vesicular glass and flight aerogel (Rietmeijer 2009b). These areas contain more Mg, Al and Ca, in variable relative proportions, than the surrounding vesicular glass (Leroux et al. 2008). The compositions of this Mg,Al,Ca-glass (Table 2) overlap somewhat with low-Fe vesicular glass (Fig. 2). Compositionally similar glass in chondritic aggregate IDP L2011A9 that serves as an analog for the smallest Wild 2

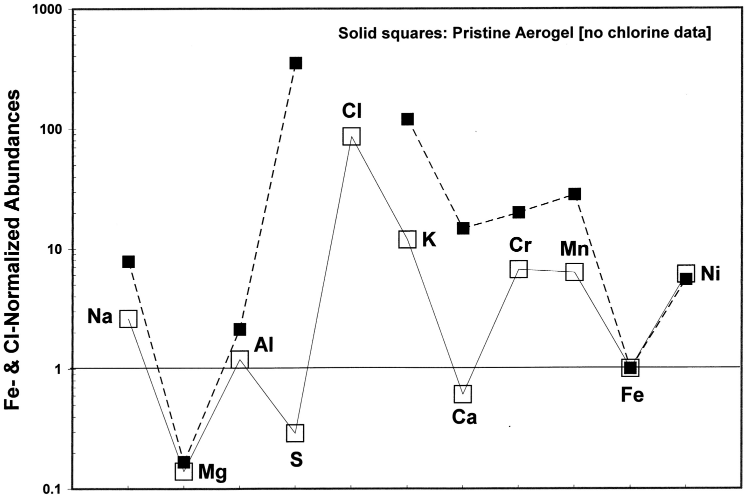

Fig. 1. Fe- and CI-normalized element abundances at percent levels measured in flight aerogel of allocation C2092,2,80,47,6 (open squares) are compared to the same element abundances at ppb levels in pristine, pre-flight, aerogel (Tsou et al. 2003). There are no data for chlorine in pristine aerogel. Reproduced from Rietmeijer (2009b) by courtesy of the Meteoritical Society.

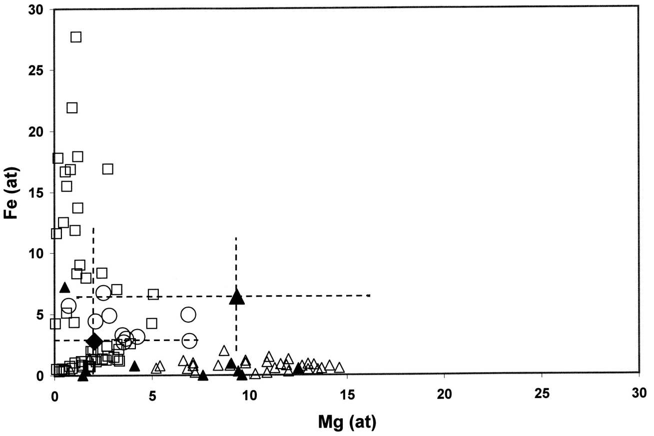

Fig. 2. Mg versus Fe (atomic %) diagram showing the mean and standard deviations of GEMS in CP IDPs (solid triangle; dashed lines) and GEMS-like objects Stardust tracks C2,7,10; C2009,2,57; FC5,0,5 and C2115,33,123,0 (solid diamond; dashed lines) (source: Ishii et al. 2008). Compositions are also shown of GEMS-like objects in allocation C2092,2,80,46,1 (open circles) and vesicular glass (open squares) (Rietmeijer 2009c). The compositions of "dust-rich areas" in vesicular glass (open triangles; Leroux et al. 2008) are shown including C2004,1,44,4,3 (solid triangles; author PET phase). The materials shown in this diagram contain mostly Si, Mg, and Fe. No flight aerogel background correction was applied to data shown in this figure.

grains (Rietmeijer 2009a) include Al-free (i.e., below the detection limit) and Al-bearing populations. The Stardust Mg,Al,Ca glass also seems to show this subdivision for the data that were not corrected for background values (see below). This glass could be "ghost-minerals or mineral assemblages" (Leroux et al. 2008) and it is tempting to compare them to the amorphous spherical grain (~250 nm) and smaller euhedral grains with Si-Ca-Mg-Al-O compositions that are compositionally similar to Ca-Mg-Al pyroxene in allocation FC4-0-3-1-1 (Tomeoka et al. 2008).

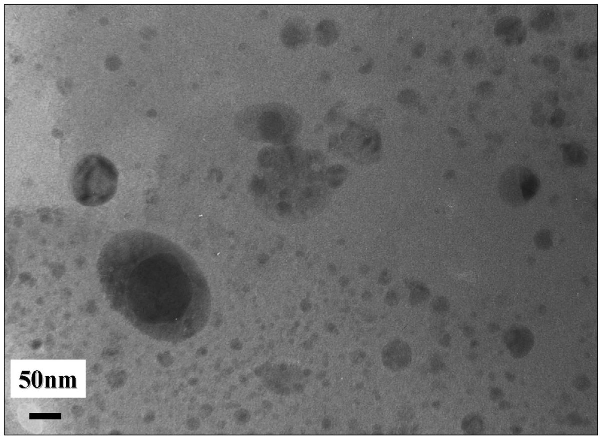

Fig. 3. Transmission electron micrograph of an area in Si-rich vesicular glass in allocation C2092,2,80,46 showing the size range of Fe-Ni-S compound inclusions, including core-rim grains (black and dark gray), and the heterogeneous distribution patterns. The object just above the center is a dense cluster of nanometer inclusions that looks like a GEMS-like object embedded glass (light gray). After background correction the inclusion-free patch of glass is pure silica.

To test a possible relationship between this glass and Wild 2 silicates, I used data from Leroux et al. (2008) that were not corrected for a flight aerogel background and silicate compositions in the analog aggregate IDP L2011A9. These silicates are (1) olivine, *mg* = 0.93-0.78, (2) Ca-free pyroxene, *mg* = 0.74 (3) low-Ca pyroxene, $En_{70}Fs_{25}Wo_{5}$, and (4) Ca-rich pyroxene with an $En_{44}Fs_{17}Wo_{39}$ composition. The silicates may contain variable minor amounts of Al, Mn and Ni; all are Cr-free (Rietmeijer 2009a). The Fe- and CI-normalized element abundances for the Al-free and Al-containing glasses are not significantly different, including C2004,1,44,4,2, and C2004,1,44,4,3 (Fig. 4). These normalized abundances also show that the glass compositions are consistent with Mg-rich olivine and pyroxenes.

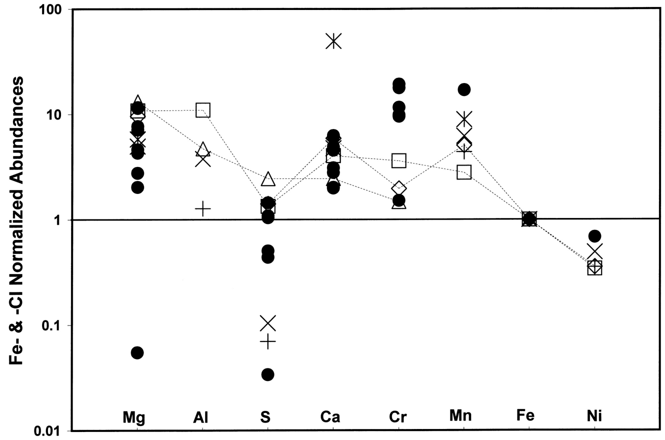

Fig. 4. Fe- and CI normalized abundances for massive glass wherein Al is below its detection limit (open diamonds) and Al-bearing (open squares) massive glass patches in Si-rich vesicular glass from several deceleration tracks, including C2004,1,44,4,2 (open triangles) obtained by element mapping (source: Leroux et al. 2008). The normalized abundance for three glass patches in allocation C2004,1,44,4,3 (dots) were obtained by AEM point analyses (source: the author, PET-phase) provide measure for the general chemical heterogeneity of these glass patches. No flight aerogel background correction was applied to Stardust data shown in this figure. The average compositions of olivine (+), Ca-free/low-Ca pyroxene (×) and Ca-rich pyroxene (*) in the analog aggregate IDP L2011A9 (Rietmeijer 2009a) are shown for comparison; the trace amounts of sulfur are associated with Fe-sulfides in the IDP.

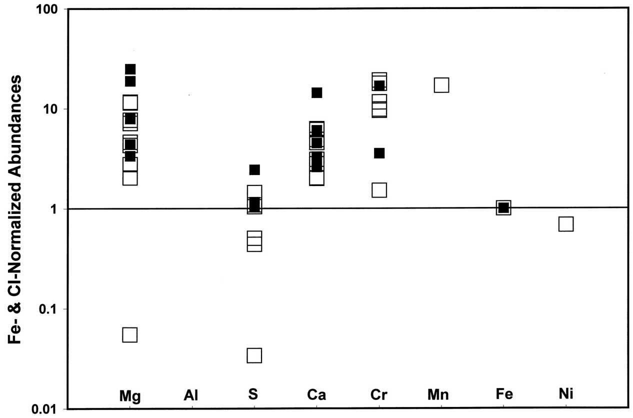

Fig. 5. Fe- and CI-normalized abundances for three massive glass patches in Si-rich vesicular glass in allocation C2004,1,44,4,3 as measured (open squares) and those corrected for the flight aerogel background (solid squares) that was determined for this sample.

The statistical data (Table 2) clearly highlight the chemical heterogeneity that is more significant for Cr, Ni, and Mn than for the other elements, which is consistent with the silicate data from the analog aggregate IDP L2011A9. The Fe versus S (at) correlation in allocation C2004,1,44,4,3 suggests that sulfur is present in tiny FeS grains. Low Cr, Ni, and Mn abundances match the flight aerogel background that was determined for this sample. The uncorrected data suggest that Ca,Mg,Al-Si and Ca,Mg-Si glasses are mixed intimately at nanometer scales.

Table 2. Mean and standard deviation (S.D.) atomic % (calculated by the author) for Al-free, that is below the detection limit, and Al-containing Mg,Al,Ca glass in four different Stardust tracks (source: Leroux et al. 2008, Table 5) The right-hand column indicates the percentage of glass wherein the element listed is below the detection limit.

	Mean	S.D.	Min.	Max.	%
			Al-free glass		
Mg	9.68	3.86	1.8	14.1	0
Si	23.82	7.61	23	30	0
S	0.68	0.68	0.21	2.0	0
Ca	0.34	0.50	0	0.77	9
Cr	0.03	0.04	0	0.11	64
Mn	0.05	0.06	0	0.20	18
Fe	0.84	0.38	0.2	2.0	0
Ni	0.02	0.02	0	0.07	55
			Al-bearing glass		
Mg	9.98	3.34	0.8	14.6	0
Al	0.80	1.12	0.19	4.5	0
Si	25.43	1.94	22	29	0
S	0.60	0.45	0.16	1.9	0
Ca	0.21	0.15	0	0.51	5
Cr	0.04	0.06	0	0.19	48
Mn	0.02	0.03	0	0.11	48
Fe	0.77	0.43	0.10	2.0	0
Ni	0.01	0.02	0	0.08	62

However, a comparison of the measured Fe- and CI-normalized abundances, and the same data but corrected for the flight aerogel background, shows Ca,Mg-Si glass in allocation C2004,1,44,4,3 (Fig. 5). After background correction four of the original data points could not be shown because Fe was present at less than its background value. It suggests small variations in already low Fe contents, which might also apply to chromium. The observations support that this massive glass could be melted comet Wild 2 silicates. The characteristic knife-sharp interfaces between mineral grains, compressed flight aerogel and Si-rich glass suggest an apparent lack of mixing during hypervelocity capture. The xenocryst-like appearance of this massive glass in Si-rich vesicular glass (cf. Leroux et al. 2008, Fig. 13) could support that they are "foreign" incandescent droplets of melted silicate and melted aerogel.

Deep metastable eutectic glass: This proposition is testable because this glass would not have a stoichiometric mineral composition but instead have higher silica contents. The compositions of two Ca,Mg-Si glass patches and a partial, amorphous rim on a forsterite grain (Table 3) show (1) essentially identical compositions despite a choice of Mg-silicates and (2) silica contents that are too high for stoichiometric olivine or pyroxene. The observed compositions (Table 3) match the smectite dehydroxylate composition that was possible by either one of two reactions:

$$3\ Mg_2SiO_4 + 5\ SiO_2 = Mg_6Si_8O_{22},\ \text{or} \qquad (1)$$

$$6\ MgSiO_3 + 2\ SiO_2 = Mg_6Si_8O_{22}. \qquad (2)$$

This deep metastable eutectic (DME) smectite dehydroxylate composition forms during vapor phase condensation of $Mg\text{-}SiO\text{-}H_2\text{-}O_2$ and $Mg\text{-}Fe\text{-}SiO\text{-}H_2\text{-}O_2$ vapors (Rietmeijer et al. 1999, 2002a). The conditions conducive to form quenched DME solids are very high temperatures and ultra-rapid cooling, which certainly applies to aerogel during 6.1 km s^{-1} hypervelocity impact at temperatures above the forsterite melting point that existed for 2 μs and may have reached 8000 K (Anderson and Cherne 2008).

In this regard, the amorphous, partial rim on a ~500 nm single-crystal olivine ($Fo_{98}Fa_2$) grain in allocation C2004,1,44,4,3 is perhaps a critical observation. The rim measured is ~450 nm thick. Its interfaces with olivine and the surrounding vesicular glass are sharp. One could propose that the rim formed when magnesium diffused from a surface melt layer on olivine to a surrounding silica phase. It constrains the temperatures during this process around the forsterite melting temperature of 1890 °C that is higher than the silica aerogel melting temperature (1727 °C). Assuming a diffusion distance of the half-width of the rim and using the effective diffusion coefficient (D) for Mg in silica at is melting point, $D = 10^{-16}\ m^2\ s^{-1}$ (Nascimento and Zanotto 2006), I calculate in the most simple way a diffusion time of 1925 μs. This diffusion time is huge in context with the first assessments of event durations in Stardust that ranged from 0.1 μs (1200 °C) to ~1 s (200 °C) for Fe-S diffusion in zoned sulfide nanograins (Rietmeijer 2008) and post-impact temperatures around 1800 °C for <0.1 μs based on MgO and SiO_2 diffusion between amorphous MgO-rich "ghost-minerals" and silica melt (Roskosz et al. 2008). To form this core-rim texture it required high temperatures above the silica and forsterite melting points; no survival of forsterite. Maybe the interpretation of the core-rim structure is incorrect, i.e., there is no temporal and genetic co-relationship between forsterite and smectite dehydroxylate glass.

The forsterite grain was part of a Wild 2 particle that produced a hedgehog-type aerogel track wherein iron silicide phases formed during hypervelocity capture at temperatures around 1500 °C (Nakamura et al. 2008b, Rietmeijer et al. 2008). This temperature was based on the Fe-silicide compositions but, and this is the case for most Stardust temperature estimates, it is based on surviving or neo-formed mineral properties. They are minimum temperatures. The bulbous part of a track, and the distorted "crater" of the hedgehog track, probably contained a mixture of vaporized aerogel, presumable as SiO vapor, incandescent molten aerogel droplets and comet material that survived, and was melted or evaporated. A less-heated grain moving down the evolving bulb could become entrained in, or encapsulated by, a wake of silica-saturated melt and vapor. In this scenario for forsterite in allocation C2004,1,44,4,3, I submit it was enclosed in a melt/vapor shell when it lodged in a volume of impact-generated Si-rich melt (~10–20 microns) that itself had penetrated hot aerogel of the track wall. Subsequent radiative heat transport from aerogel to the glass smoothed small chemical and textural heterogeneities that remained from the capture process, including the removal of vesicles in glass rims. The unique DME smectite dehydroxylate compositions (Table 3) reflect the fact that the bulk system (melt, vapor or both) will always be silica saturated. To form glass with a deep metastable eutectic composition the melt and vapors had to be quenched very rapidly from very high temperatures above the liquidus at ~1500 °C in the $MgO\text{-}SiO_2$ system (cf. Rietmeijer et al. 2002a). $Mg\text{-}SiO\text{-}H_2\text{-}O_2$ and $Mg\text{-}Fe\text{-}SiO\text{-}H_2\text{-}O_2$ vapor condensation experiments showed how a few water molecules present in the condensation chamber caused hydration of the condensed $Mg_6Si_8O_{22}$ phase to form rare smectite proto-phyllosilicates (Rietmeijer et al. 2002b). It is suggested that when some of few gas phase H_2O molecules in the Stardust collector were able to intact with $Mg_6Si_8O_{22}$ glass, smectite proto-phyllosilicates might have formed in Stardust glass of this particular composition. They will be very small and extremely rare.

Table 3. Compositions (wt% oxides) of two massive Ca,Mg-Si glass patches, and a partial amorphous rim around a forsterite grain (cf. Leroux et al. 2008, Fig. 17a) embedded in the Si-rich vesicular glass in Stardust allocation C2004,1,44,4,3 (author, PET phase).

	MgO	SiO_2	CaO
Patch 1	21.3	77.8	0.9
Patch 2	27.6	71.5	0.9
Rim	19.1	80.9	0

INDIGENOUS COMET GLASS

Stardust allocation (C2115-24-22-1-8) is a ~5.4 μm × 4.6 μm particle (Tomeoka et al. 2008, Fig. 7) of shattered Mg-rich olivine, diopside and shards of massive Si-O-Al glass with minor, variable amounts of Na, Mg, and K. The glass contains few vesicles (Tomeoka et al. 2008, Fig. 5b). There are no quantitative chemical data available for this "indigenous comet glass" (Tomeoka et al. 2008). The particle size and shattered appearance suggest it was embedded along a track stylus. It was not melted during capture but it was probably rapidly heated and quenched. The shattered appearance is an artifact of the ultra-microtome process to prepare Stardust samples for TEM analyses. The rapidly heated and quenched mineral grains will shatter along a dominant crystallographic plane after experiencing structural weakening caused by ultra rapid heating and expansion of the unit cell to temperatures below the melting point and followed by rapid cooling and contraction (Rietmeijer 2004b). While the authors suggest a link to chondrule mesostasis, I note that the analog aggregate IDP L2011A9

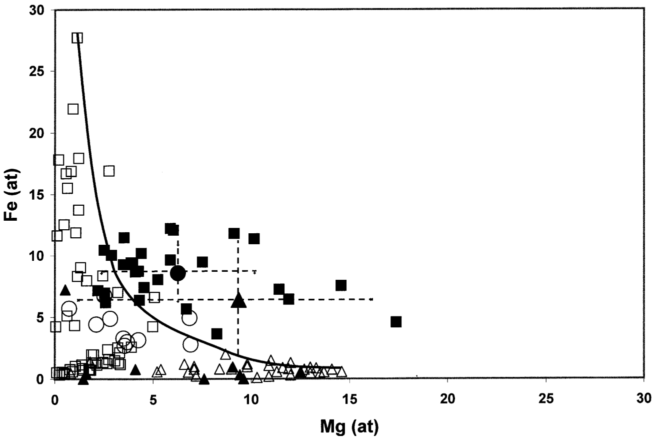

Fig. 6. The same Mg versus Fe (atomic %) diagram as Fig. 2 showing the mean and standard deviations for GEMS in six chondritic aggregate IDPs (solid triangle; dashed lines; source: Ishii et al. 2008) and the low porosity chondritic aggregate IDP L2011A9 (dot; dashed lines) that is used as an analog for nanometer scale Wild 2 particles (Rietmeijer 2009a). The latter mean and S.D. atomic % are listed in (Table 4). The solid line separates GEMS from glasses that are attributable to Wild 2 particles, except "indigenous comet glass" wherefore no data are available.

contains a 2 µm × ~1 µm amorphous silica glass with variable Mg, Al and Ca contents but no Na or K, and diopside, $En_{50}Fs_2Wo_{48}$ (Rietmeijer 2009a). The chondritic aggregate IDPs typically contain very little Na and K, if any (Rietmeijer 1998).

DISCUSSION AND CONCLUSIONS

What can be summarized as a working hypothesis for the continued analyses of Stardust samples? First, "indigenous comet glass" appears to have survived but its origins are uncertain. There are two possibilities: (1) glass from the inner solar system that survived radial transport into the Kuiper belt zone, and (2) glass from the solar nebula accretion regions of the cometary, chondritic aggregate IDPs. Indigenous comet glass is probably better preserved in the stylus of a deceleration track than in its upper bulbous part.

Second, indigenous comet GEMS will not be recognizable unless they survived with an embedded relict grain. The search for GEMS will continue but I submit that the term "GEMS-like objects" will no longer be used in Stardust sample analysis. Their look-alikes in Si-rich glass are a textural artifact or caused by a comet pyrrhotite grain such as was demonstrated by Ishii et al (2008) for GEMS-like objects in compressed flight aerogel. Sulfides in analog IDPs IDP L2011A9 are mostly a few nanometers to ~500 nm in size with few one micron grains (Rietmeijer 2009a). The GEMS like objects are a mixture of melted and modified comet pyrrhotite grains and melted contaminated flight aerogel. Their compositions are restricted to the part below the solid curve in the Mg versus Fe (at) diagram (Fig. 6) where they overlap with Si-rich vesicular glass compositions (Figs. 2 and 6). While the area below the curve in Fig. 6 that separates GEMS and modified Wild 2 particles includes GEMS compositions in six chondritic aggregate IDPs, their means are higher in Mg and Fe and their silica contents are less than in GEMS-like objects. Using the analog IDP L2011A9 for the smallest comet Wild 2 particles, their chemical signatures preserved in vesicular glass support a mixture of GEMS, amorphous Mg,Fe-silicates, forsterite, perhaps enstatite, and Fe,Ni-sulfides (Rietmeijer 2009a, 2009b, 2009c).

Table 4. Mean and standard deviation (S.D.) atomic % for 27 GEMS in chondritic aggregate IDP L2011A9; ~40% of these GEMS are Ca-free (Rietmeijer 2009a)

	Mean ± S.D.
Mg	6.27 ± 3.90
Al	1.85 ± 1.24
Si	16.62 ± 3.07
S	3.72 ± 2.15
Ca	0.29 ± 0.21
Fe	8.56 ± 2.29
Ni	0.63 ± 0.54

Third, some fraction of the indigenous comet silicates were melted, were perhaps even vaporized. The low-Ca Mg-glass (after background correction) and Si-O-Al glass inclusions (Figs. 2 and 6) in the Si-rich vesicular glass are probably melted silicates. There are two caveats to consider: (1) there are still but very few quantitative analyses available and (2) the data are not corrected for a flight aerogel background composition. When properly corrected, the glass has a deep metastable eutectic, smectite-dehydroxylate composition with traces of Fe and Ca. This magnesiosilica composition is the result of assimilation of Mg-rich forsterite and enstatite from comet Wild 2 and silica melt and SiO vapor. The DME glass compositions indicate a sudden sharp rise to very high temperatures followed by ultra-rapid quenching in the bulbous part of deceleration tracks. In the silica saturated conditions Wild 2 mineral melts cannot preserve the original, stoichiometric mineral composition. Instead it will have a specific deep metastable eutectic composition. Most glass will be Mg-rich but there is no chemical constraint as DME dehydroxylate compositions can form in many chemical systems relevant to primitive dust compositions (Nuth et al. 2000b, 2002). I predict that when DME glass compositions in Stardust can be proven to be a recurring phenomenon, there is still a wealth of information on the smallest Wild 2 minerals hidden in these glasses. This knowledge will be necessary and invaluable.

Acknowledgments—I am indebted to Dr. Bill Anderson at LANL for patience explaining aerogel behavior during the collection of Wild 2 particles. I thank George Flynn and an anonymous reviewer for their constructive reviews. This work was supported by grant NNX07AM65G through the NASA Stardust Analyses Program.

Editorial Handling—Dr. Scott Sandford

REFERENCES

Anderson W. W. and Cherne F. J. 2008. Model development for assessment of thermal histories of returned stardust cometary dust samples (abstract #2540). 39th Lunar and Planetary Science Conference. CD-ROM.

Bradley J. P. 1994. Chemically anomalous, pre-accretionally irradiated grains in interplanetary dust from comets. *Science* 265: 925–929.

Bradley J. P. and Brownlee D. E. 1986. Cometary particles: Thin sectioning and electron beam analysis. *Science* 231:1542–1544.

Bradley J. P. and Ishii H. A. 2008. Comment on "The shape and composition of interstellar silicate grains." *Astronomy & Astrophysics* 486:781–784.

Bradley J. P., Sandford S. A., and Walker R. M. 1988. Interplanetary dust particles. In *Meteorites and the early solar system*, edited by Kerridge J. F. and Matthews M. S. Tucson: The University of Arizona Press. pp. 861–898.

Bradley J. P., Snow T., Brownlee D. E., Keller L. P., Flynn G. J., and Miller M. 1998. Optical, mineralogical, and trace element properties of GEMS: Evaluating the interstellar connection (abstract #1737). 29th Lunar and Planetary Science Conference. CD-ROM.

Brownlee D. E. 1978. Interplanetary dust: Possible implications for comets and presolar interstellar grains. In *Protostars and planets*, edited by Gehrels T. Tucson: The University of Arizona Press. pp. 134–150.

Brownlee D. E. 1985. Cosmic dust: Collection and research. *Annual Review Earth and Planetary Science* 13:147–173.

Brownlee D. E. and Joswiak D. J. 2004. The solar nebula's first accretionary particles (FAPs)—Are they preserved in collected interplanetary dust samples? (abstract #1944). 35th Lunar and Planetary Science Conference. CD-ROM.

Brownlee D. E., Joswiak D. J., Bradley J. P., and Matrajt G. 2007. The origin of crystalline silicates in comets and large scale mixing in the solar nebula (abstract # 2189). 38th Lunar and Planetary Science Conference. CD-ROM.

Brownlee D. E., Joswiak D. J., Love S. G., Bradley J. P., Nier O. A., and Schlutter D. J. 1994. Identification and analysis of cometary IDPs (abstract). 25th Lunar and Planetary Science Conference. pp. 185–186.

Brownlee D. E., Joswiak D. J., Schlutter D. J., Pepin R. O., Bradley J. P., and Love S. G. 1995. Identification of individual cometary IDPs by thermally stepped He release (abstract). 26th Lunar and Planetary Science Conference. pp. 183–184.

Brownlee D., Tsou P., Aléon J., Alexander, C. M. O'D., Araki T., Bajt S. Baratta G. A., Bastien R., Bland Ph., Bleuet P., Borg J., Bradley J. P., Brearley A., Brenker F., Brennan S., Bridges J. C., Browning N. D., Brucato J. R., Bullock E., Burchell M. J., Busemann H., Butterworth A., Chaussidon M., Cheuvront A., Chi M., Cintala M. J., Clark B. C., Clemett S. J., Cody G., Colangeli L., Cooper G., Cordier P., Daghlian C., Dai Z., D'Hendecourt L., Djouadi Z., Dominguez G., Duxbury T., Dworkin J. P., Ebel D. S., Economou T. E., Fakra S., Fairey S. A. J., Fallon S., Ferrini G., Ferroir T., Fleckenstein H., Floss C., Flynn G., Franchi I. A., Fries M., Gainsforth Z., Gallien J.-P., Genge M., Gilles M. K., Gillet P., Gilmour J., Glavin D. P., Gounelle M., Grady M. M., Graham G. A., Grant P. G., Green S. F., Grossemy F., Grossman L., Grossman J. N., Guan Y., Hagiya H., Harvey R., Heck P., Herzog G. F., Hoppe P., Hörz F., Huth J., Hutcheon I. D., Ignatyev K., Ishii H., Ito M., Jacob D., Jacobsen C., Jacobsen S., Jones S., Joswiak D., Jurewicz A., Kearsley A. T., Keller L. P., Khodja H., Kilcoyne A. L. D., Kissel J., Krot A., Langenhorst F., Lanzirotti A., Le L., Leshin L. A., Leitner J., Lemelle L., Leroux H., Liu M-C., Luening K., Lyon I., MacPherson G., Marcus M.A., Marhas K., Marty B., Matrajt G., McKeegan K., Meibom A., Mennella V., Messenger K., Messenger S., Mikouchi T., Mostefaoui S., Nakamura T., Nakano T., Newville M., Nittler L. R., Ohnishi I., Ohsumi K., Okudaira K., Papanastassiou D. A., Palma R., Palumbo M. E., Pepin R. O, Perkins D., Perronnet M., Pianetta P., Rao W., Rietmeijer F. J. M., Robert F., Rost D., Rotundi A., Ryan R., Sandford S. A., Schwandt G. S., See T. H., Schlutter D., Sheffield-Parker J., Simionovici A., Simon S., Sitnitsky I., Snead C. J., Spencer M. K., Stadermann F., Steele A., Stephan T., Stroud R., Susini J., Sutton S. R., Suzuki Y., Taheri M., Taylor S., Teslich N., Tomeoka K., Tomioka N., Toppani A., Trigo-Rodríguez J. M., Troadec D., Tsuchiyama A., Tuzzolino A. J., Tyliszczak T., Uesugi K., Velbel M., Vellenga J., Vicenzi E., Vincze L., Warren J., Weber I., Weisberg M., Westphal A. J., Wirick S., Wooden D., Wopenka B., Wozniakiewicz P., Wright I., Yabuta H., Yano H., Young E. D., Zare R. N., Zega T., Ziegler K., Zimmerman L., Zinner E., and Zolensky M. 2006. Comet 81P/Wild 2 under a microscope. *Science* 314:1711–1716.

Ciesla F. J. 2007. Outward transport of high-temperature materials around the midplane of the solar nebula. *Science* 318:613–615.

Fabian D., Jäger C., Henning Th., Dorschner J., and Mutschke H. 2000. Steps toward interstellar silicate mineralogy V. Thermal evolution of amorphous magnesium silicates and silica. *Astronomy & Astrophysics* 364:282–292.

Hallenbeck S. L., Nuth III, J. A., and Daukantes P. L. 1998. Mid-infrared spectral evolution of amorphous magnesium silicate smokes annealed in vacuum: Comparison to cometary spectra. *Icarus* 131:198–209.

Hörz H., Bastien R., Borg J., Bradley J. P., Bridges J. C., Brownlee D. E, Burchell M. J., Chi M., Cintala M. J., Dai Z. R., Djouadi Z., Dominguez G., Economou T. E., Fairey S. A. J., Floss C., Franchi I. A., Graham G. A, Green S. F., Heck P., Hoppe P., Huth J., Ishii H., Kearsley A. T., Kissel J., Leitner J., Leroux H., Marhas K., Messenger K., Schwandt C. S., See T. H., Snead C., Stadermann F. J., Stephan T., Stroud R., Teslich N., Trigo-Rodríguez J. M., Tuzzolino A. J., Troadec D., Tsou P., Warren J., Westphal A., Wozniakiewicz P., Wright I., and Zinner E. 2006. Impact features on Stardust: Implications for comet 81P/Wild 2 dust. *Science* 314:1716–1719.

Hsieh H. H. and Jewitt D. 2006. A population of comets in the main asteroid belt. *Science* 312:561–563.

Ishii H. A., Bradley J. P., Dai Z. R., Chi M., Kearsley A. T., Burchell M. J., Browning N. D., and Molster F. 2008. Comparison of comet 81P/Wild 2 dust with interplanetary dust from comets. *Science* 319:447–450.

Joswiak D. J., Brownlee D. E., Pepin R. O., and Schlutter D. J. 2000. Characteristics of asteroidal and cometary IDPs obtained from stratospheric collections: Summary of measured He release temperatures, velocities and descriptive mineralogy (abstract #1500). 31st Lunar and Planetary Science Conference. CD-ROM.

Keller L. P. and Messenger S. 2004. On the origin of GEMS (abstract #1985). 35th Lunar and Planetary Science Conference. CD-ROM.

Keller L. P., Bajt S., Baratta G. A., Borg J., Bradley J. P., Brownlee D. E., Busemann H., Brucato J. R., Burchell M., Colangeli L., D'Hendecourt L., Djouadi Z., Ferrini G., Flynn G., Franchi I. A., Fries M., Grady M.M., Graham G. A, Grossemy F., Kearsley A., Matrajt G., Nakamura-Messenger K, Mennella V., Nittler L., Palumbo M. E., Stadermann F. J., Tsou P., Rotundi A., Sandford S. A., Snead C., Steele A., Wooden D., and Zolensky M. 2006. Infrared spectroscopy of comet 81P/Wild 2 samples returned by Stardust. *Science* 314:1728–1731.

Leroux H., Rietmeijer F. J M., Velbel M. A., Brearley A. J., Jacob D., Langenhorst F., Bridges J. C., Zega T. J., Stroud R. M., Cordier P., Harvey R. P., Lee M., Gounelle M., and Zolensky M. E. 2008. A TEM study of thermally modified comet 81P/Wild 2 dust particles by interactions with the aerogel matrix during the Stardust capture process. *Meteoritics & Planetary Science* 43:97–120.

Lisse C. M., VanCleve J., Adams A. C., A'Hearn M. F., Fernández Y. R., Farnham T. L., Armusm L., Grillmair C. J., Ingalls J., Belton M. J. S., Groussin O., McFadden L. A., Meech K. J., Schultz P. H., Clark B. C., Feaga L. M., and Sunshine J. M. 2006. Spitzer spectral observation of the Deep Impact ejecta. *Science* 313:635–640.

Mackinnon I. D. R. and Rietmeijer F. J. M. 1987. Mineralogy of chondritic interplanetary dust particles. *Reviews in Geophysics* 25:1527–1553.

Martin P. G. 1995. On the value of GEMS (glass with embedded metal and sulphides). *The Astrophysical Journal* 445:L63–L66.

Min M., Waters L. B. F. M., de Koter A., Hovenier J. W., Keller L. P., and Markwick-Kemper F. 2007. The shape and composition of interstellar silicate grains. *Astronomy & Astrophysics* 462:667–676.

Nascimento M. L. F. and Zanotto E. D. 2006. Mechanisms and dynamics of crystal growth, viscous flow, and self-diffusion in silica glass. *Physical Review B* 73:024209-1–024209-7.

Nakamura T, Noguchi T. Tsuchiyama A., Ushikubo T., Kita N. T., Valley J. W., Zolensky M. E., Kakazu Y., Sakamoto K., Mashio E., Uesugi K., and Nakano T. 2008a. Chondrule like objects in short-period comet 81P/Wild 2. *Science* 321:1664–1667.

Nakamura T., Tsuchiyama A., Akaki T., Uesugi K., Nakano T., Takeuchi A., Suzuki Y., and Noguchi T. 2008b. Bulk mineralogy and three-dimensional structures of individual Stardust particles deduced from synchrotron X-ray diffraction and microtomography analysis. *Meteoritics & Planetary Science* 43:247–259.

Nuth III, J. A., Hill H. G. M., and Kletetschka G. 2000a. Determining the ages of comets from the fraction of crystalline dust. *Nature* 406:275–276.

Nuth III, J. A., Hallenbeck S. L., and Rietmeijer F. J. M. 2000b. Laboratory studies of silicate smokes: Analog studies of circumstellar materials. *Journal of Geophysical Research* 105(A5): 10:387–10,396.

Nuth III J. A., Rietmeijer F. J. M., and Hill H. G. M. 2002. Condensation processes in astrophysical environments: The composition and structure of cometary grains. *Meteoritics Planetary Science* 37:1579–1590.

Rietmeijer F. J. M. 1998. Interplanetary dust particles. In *Planetary materials*, edited by Papike J. J. Reviews in Mineralogy, vol. 36. Chantilly, Virginia: Mineralogical Society of America. pp. 2-1–2-95.

Rietmeijer F. J. M. 2000. Interrelationships among meteoric metals, meteors, interplanetary dust, micrometeorites, and meteorites. *Meteoritics & Planetary Science* 35:1025–1041.

Rietmeijer F. J. M. 2002. The earliest chemical dust evolution in the solar nebula. *Chemie der Erde* 62:1–45.

Rietmeijer F. J. M. 2004a. Interplanetary dust and carbonaceous meteorites: Constraints on porosity, mineralogy and chemistry of meteors from rubble-pile planetesimals. *Earth, Moon, and Planets* 95:321–338.

Rietmeijer F. J. M. 2004b. Dynamic pyrometamorphism during atmospheric entry of large (~10 micron) pyrrhotite fragments from cluster IDPs. *Meteoritics & Planetary Science* 39:1869–1887.

Rietmeijer F. J. M. 2008. Time, temperatures, and pressure indicated by metastable iron-sulfide nanophases in melted Stardust aerogel (abstract #1188). 39th Lunar and Planetary Science Conference. CD-ROM.

Rietmeijer F. J M. 2009a. A cometary aggregate interplanetary dust particle as an analog for comet Wild 2 grain chemistry preserved in silica-rich Stardust glass. *Meteoritics & Planetary Science* 44: 1589–1609.

Rietmeijer F. J. M. 2009b. Chemical identification of comet 81P/Wild 2 dust after interacting with molten silica aerogel. *Meteoritics & Planetary Science* 44:1121–1132.

Rietmeijer F. J. M. 2009c. Corrected chemical signatures in Stardust glass reveal Wild 2 particles that resemble matrix grains of aggregate IDPs (abstract #1189). 40th Lunar and Planetary Science Conference. CD-ROM.

Rietmeijer F. J. M. and Nuth III J. A. 2007. Laboratory simulation of Mg-rich ferromagnesiosilica dust: The first building blocks of comet dust. *Advances in Space Research* 39:351–357.

Rietmeijer F. J. M., Nuth III J. A. and Karner J. M. 1999. Metastable eutectic condensation in a Mg-Fe-SiO-H_2-O_2 vapor: Analogs to circumstellar dust. *The Astrophysical Journal* 527:395–404.

Rietmeijer F. J. M., Nuth III J. A., Karner J. M. and Hallenbeck S. L. 2002a. Gas to solid condensation in a Mg-SiO-H_2-O_2 vapor: Metastable eutectics in the MgO–SiO_2 phase diagram. *Physical Chemistry Chemical Physics* 4:546–551.

Rietmeijer F. J. M., Hallenbeck S. L., Nuth III J. A., and Karner J. M. 2002b. Amorphous magnesiosilicate smokes annealed in vacuum: The evolution of magnesium silicates in circumstellar and cometary dust. *Icarus* 156:269–286.

Roskosz M., Leroux H., and Watson H. C. 2008. Thermal history, partial preservation and sampling bias recorded by Stardust cometary grains during their capture. *Earth Planetary Science Letters* 273:195–202.

Tomeoka K., Tomioka N., and Ohnishi I. 2008. Silicate minerals and Si-O glass in comet Wild 2 samples: Transmission electron microscopy. *Meteoritics & Planetary Science* 43:273–284.

Tsou P., Brownlee D. E., Hörz F., Sandford S. A., and Zolensky M. E. 2003. Wild 2 and interstellar sample collection and Earth return. *Journal of Geophysical Research* 108:E8113.

Zolensky M. E., Zega T. J., Yano H., Wirick S., Westphal A. J., Weisberg M. K., Weber I., Warren J. L., Velbel M. A., Tsuchiyama A., Tsou P., Toppani A., Tomioka N., Tomeoka K., Teslich N., Taheri M., Susini J., Stroud R., Stephan T., Stadermann F. J., Snead C. J., Simon S. B., Simionovici A., See T. J., Robert F., Rietmeijer F. J. M., Rao W., Perronnet M. C., Papanastassiou D. A., Okudaira K., Ohsumi K., Ohnishi I., Nakamura-Messenger K., Nakamura T., Mostefaoui S., Takashi Mikouchi T., Meibom A., Matrajt G., Marcus M. A., Leroux H., Lemelle L., Le L., Lanzirotti A., Langenhorst F., Krot A. N., Keller L. P, Kearsley A. T., Joswiak D., Jacob D., Ishii H., Harvey R., Hagiya K., Grossman L., Grossman J. N., Graham G. A., Gounelle M., Gillet P., Genge M. J., Flynn G., Ferroir T., Fallon S., Ebel D.S., Dai Z., Cordier P., Clark B., Chi M., Butterworth A. L., Brownlee D.E., Bridges J.C., Brennan S., Brearley A., Bradley J. P., Bleuet P., Bland P. A., and Bastien R. 2006. Mineralogy and petrology of comet Wild 2 nucleus samples. *Science* 314:1735–1739.

Zolensky M., Nakamura-Messenger K., Sverdrup J., Rietmeijer F., Leroux H., Mikouchi T., Ohsumi K., Simon S., Grossman L., Stephan T., Weisberg M., Velbel M., Zega T., Stroud R., Tomeoka K., Ohnishi, I., Tomioka N., Nakamura T., Matrajt G., Joswiak J., Brownlee D., Langenhorst F., Krot A., Kearsley A., Ishii H., Graham G., Dai Z. R., Chi M., Bradley J., Hagiya K., Gounelle M., and Bridges J. 2008. Comparing Wild 2 particles to chondrites and IDPs. *Meteoritics & Planetary Science* 43:261–272.